Innovative force sensor for indoor climbing holds – real-time measurements and data processing, design and validation

Innovative force sensor for indoor climbing holds - real time measurements and data processing, design and validation

Daniela Maffiodo [1], Raffaella Sesana [1*], Stefano Gabetti[1], Alessandro Colombo[2],

[1] *Dimeas, Politecnico di Torino, Corso Duca degli Abruzzi 24, 10129 Torino, Italy*
[2] *DEIB, Politecnico di Milano, via Ponzio 34/5, 20133 Milano, Italy*

Abstract
In the present paper, a system to measure the evolution of load in time and space during indoor climbing is described. The system is based on a set of dedicated multiaxial load cells, which measure the load on each hold of an indoor climbing wall. When the climber hangs on a hold, the load signal is read and sent to a digital acquisition and processing system (DAQ). Sensor design allows for measurement of the force components applied to the climbing holds, regardless of the application point of the force on the hold. Local deformations were measured through strain gauges. Based on the electrical configuration of the strain gauges, the values of the applied forces can be computed, making the contributions to the deformation due to bending moments and torsion negligible. The sensor was designed assuming a maximum applicable load of 200 kg without plastic deformation. The design process was based on both analytical and finite element method (FEM) analyses. An experimental calibration and testing campaign was performed to validate the sensor design.

Keywords
Load cell, indoor climbing, real time force measurement, sensor, design

1. Introduction

Climbing is a complex activity that involves strength, balance, and dynamic coordination of the lower and upper body. Constant practice can improve the performance of a climber. A very experienced climber can typically only complete a perfect execution of a climbing sequence after several cycles of trial and error with macroscopic changes in efficiency, obtained by means of small variations in posture, such as the positioning of a single finger. Quantitative indicators that measure and follow the performance evolution with training are scarce, both in the sport technical and in the biomechanic literature. During sport activity, the climber interacts only with the climbing holds. The measurement of the forces and moments exchanged with the holds and the force-time profile can be used to gain a quantitative assessment of the climbing performance. To this aim, specialised sensors, as well as suitable biometric parameters representative of the climbing activity, are needed.

* corresponding author: raffaella.sesana@polito.it

Some attempts to measure and process quantitative data on climbing performance were made in the past. In studies by Quaine et al. [1, 2], the authors measured the forces exerted on climbing holds to investigate the mechanisms exploited by the body to control equilibrium during climbing activity, in particular how forces are redistributed between contacting hands and feet when one contact is removed.

Noe et al. [3, 4] discussed the anticipatory postural adjustments (APAs) associated with a voluntary rocking on heels movement performed in a self-paced manner. In particular, ground reaction forces and the electromyographic (EMG) activity of the leg muscles were recorded to characterize the mechanisms that control the postural adjustments during climbing. Braghini et al. [5] compared the force-time histories, normalized on athletes' weight, to estimate the different performances during training and competition in speed climbing. Preloads and peak forces are the performance indices.

Fuss and Niegl [6] confirmed the time history of force exerted on the hold by the athlete as a performance parameter. In particular, the following parameters are selected as indicators of athlete's performance: peak value of the contact force, contact time, impulse, smoothness factor (defined as the ratio between parabolic approximation of force-time signal and actual one), ratio between the tangential and normal force (called friction coefficient), continuity of the movement of the centre of pressure and Hausdorff dimension. This last parameter measures the entropy of the signal and its geometrical complexity. All these parameters were obtained by means of processing force signals measured on the holds.

A similar analysis with the same parameters is reported by the same Fuss and Niegl [7]. Unfortunately, the device for force measurement implemented in this research is costly and difficult to implement in an indoor training facility. An instrumented climbing hold device was invented by Delachanal and Garnier [8] by equipping a climbing wall with force sensors. Each hold of the wall was instrumented with a force sensor positioned on the rear part of the wall. The strain gauges are positioned on a flange parallel to the wall in a radial and circumferential direction. In the patent description, it is not clear how it is possible, based on strain gauge positioning, to quantify and distinguish the force components. Furthermore, with this configuration of the strain gauges, the force applied to the hold could be partially discharged on the wall, avoiding a correct quantitative measurement. Finally, the use of a single strain gauge to measure a force component does not amplify the signal, nor reduce the signal disturbing components, nor does it allow sufficient signal resolution to measure small loads, such as the low stress exerted by children. The measuring system proposed by Lechner et al. [9] is similar to the one by Fuss and Niegl [6, 7] and provides sensors which can measure three components of force. The measuring system consisted of three uniaxial load cells integrated in a climbing hold. This solution, however, presents the disadvantage of adding measuring devices to the holding equipment, thus increasing the volume of the climbing devices, which may alter the characteristics of the climbing wall. Another application of force sensors in climbing activity is presented by Fuss and Niegl [10]. In this application, simple force sensors are used to estimate hand and foot forces exerted on holds in a climbing technique (two handed dyno). The measuring system presented in the paper is very simple and only simple testing configuration can be investigated.

In the literature, additional systems are described, that are dedicated to obtaining force

and other useful information about the climbing activity. For example, Tsang [11] proposed a climbing hold activated by static electricity of the human body. In particular, a sheet of conductive material embedded in the hold detects the contact with the climber's body, thanks to the static current discharge instantaneously produced. This information allows for recording the sequence of time instants when the athlete touches each hold and tracing the athlete's path on the wall.

In the present paper, the authors introduce an integrated climbing hold sensor that can measure the 3D force vector and acquire and process the force-time profile applied to the hold by the athlete. The proposed system does not interfere with the climber during exercise, so as not to alter the sporting experience.

Using the data collected by these sensors, it is possible to evaluate the user's performance for the purposes of sports training, rehabilitation, or psychomotricity. As will be discussed later, measurement time, rate and accuracy are sufficient to compute the position of the Center of Mass (COM) of the athlete in time. The estimation of the COM trajectory of the entire body is of great importance, as it enables simplification in the study of articulated movements. Low cost implementation, high sensibility, and versatility are the main advantages of the proposed solution. In particular, the system requirements are listed. Then the device design basics are presented and the preliminary dimensioning is validated and optimized by means of FEM analysis. Subsequently, the prototypes are manufactured and a basic climbing wall is instrumented. The measuring system is built, the validation of the measuring procedure is set up and validated. Finally, the basics for performance indicator processing are implemented and validated, both with experimental and literature data.

2. System requirements

The objective of this study was to measure the 3D vector force on each hold with high time resolution and accuracy, without interfering with the climber's perception of the wall, by introducing a sensing device as the support between the hold and the wall. The main system requirements included the following:

- sensor mechanical properties, since the sensor had to withstand the load of the climber without perceptible deformation
- sensor geometry, which had to allow embedding the sensor in the wall without leaving any visible trace on the climber's side
- measurement resolution and accuracy, which are dependent on the data acquisition board characteristics, affected by electrical and thermal noise, and influenced by nonidealities of the sensor's deformations
- measurement time resolution (dependent on the data acquisition board)

In addition, the study sought to design a sensor of minimal cost, so as to equip a whole climbing wall at a reasonable price.

The average weight of a climber was assumed to be 70 kg. Each climbing hold had to be able to bear all the load applied by one person hung by one hand. To safely account for dynamic load, a dynamic load factor of 3, which is the athlete's weight multiplication factor due to dynamic activity, was assumed. The maximum load that the sensor must safely bear

in any direction is thus 2000 N. Regarding the legal requirements on the mechanical properties of a climbing hold, note that even though in UNI EN 12572 Standard [12] the maximum loads which the hold is required to withstand are defined relative to the dimension of the hold, nothing is required regarding the hold supporting system.
In terms of resolution and accuracy, a 10 N minimum was the goal. Design requirements assumed that nonlinearities, electrical and thermal noise, cross-talk between sensing axes, and dependence of force on the point of application would not affect the measurement by more than this threshold.
The envisaged system consists of several climbing holds with embedded tri-axial load cells. Each hold is equipped with a custom-build data acquisition system (DAQ), which sends data to a central processing unit. The system thus consists of three separate components: a mechanical sensor, a data acquisition system, and the central processing unit (Figure 1).

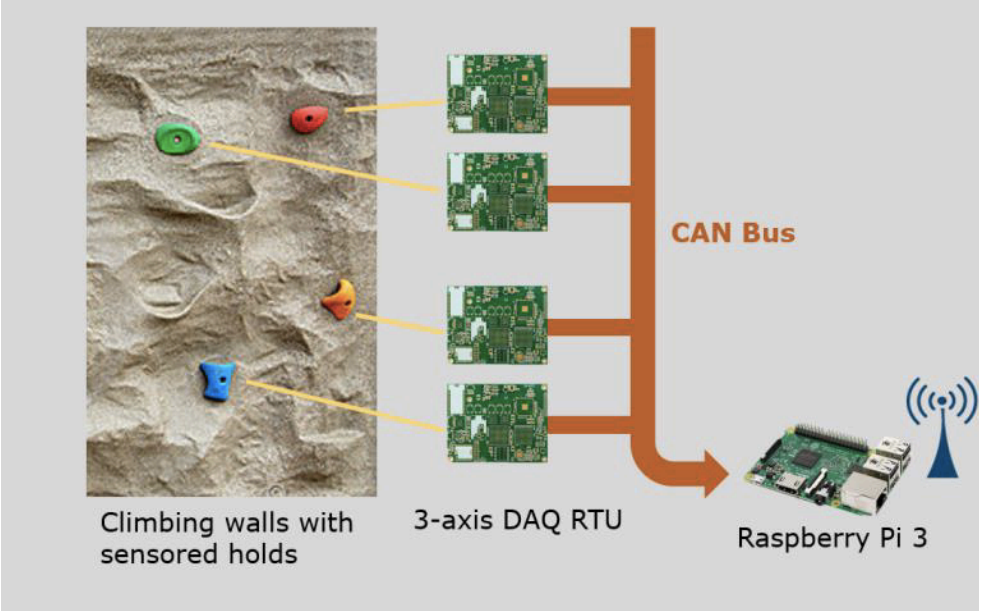

Figure 1: System architecture

3. Materials and methods

The following section contains information regarding the force sensor design, FEM analysis, DAQ, procedure to compute the COM position, and some performance indicators.

3.1. Force sensor design

The sensor, depicted in Fig. 2, supports the hold on the climbing wall. The mechanical design of the sensor, focused on in plane force measurement, was inspired by cantilever beams loaded on the free edge with a load generally not aligned with the beam axis (Figure 2*a*). The beam cross-section is circular. Strain gauges measure the deformation of the beam, which in linear regime are proportional to applied forces, according to beam elastic theory presented by Timoshenko [13]. A dedicated gauge bridge configuration eliminates the influence of the force application point. For out of plane force measurement, a dedicated

component is subjected to compression and the corresponding deformation can be related to out of plane force. Compression stiffness is different from bending stiffness and then different materials are required to fulfil general system design requirements. The out of plane force sensor was designed with a peak based material. Details are available in the dedicated patent [14].

Given a reference system on the beam, as indicated in Figure 2*b*, the external load can be split into three components: the component parallel to the beam axis (*Fz*) gives axial tensile loads; the other two components (*Fx* and *Fy*), which are parallel to the climbing wall, give shear forces and bending moments. In case the force application point is eccentric with respect to beam axis, a torque component arises, contributing a further bending moment component.

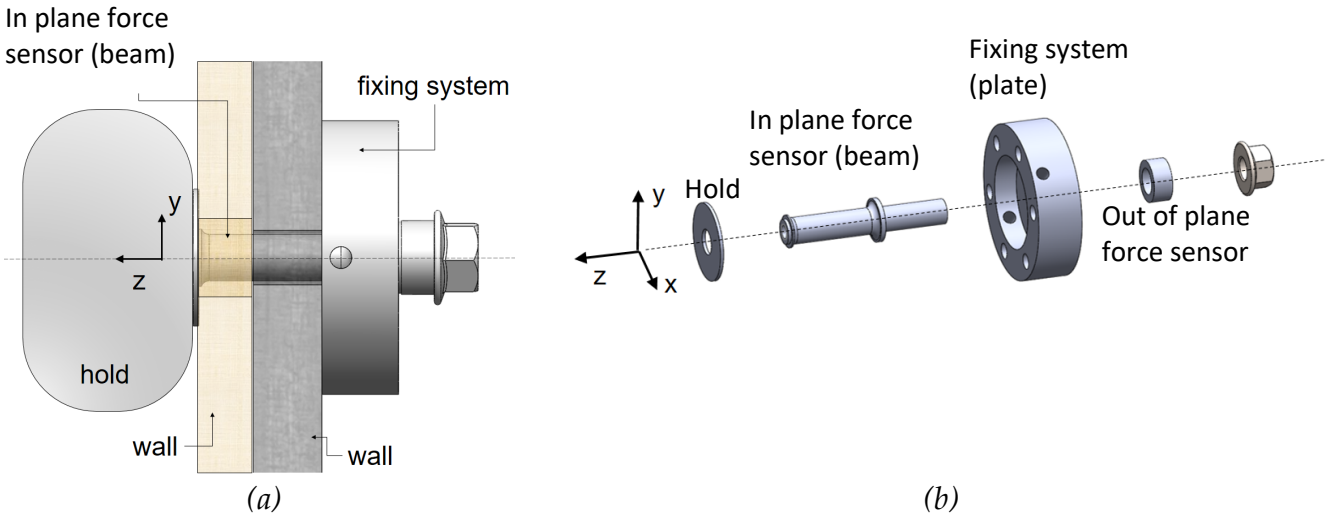

Figure 2: Sensor positioning on the climbing wall and corresponding reference system

Preliminary calculations were performed to determine the beam reference dimensions, with requirements related to structural considerations (static and dynamic load generated by the climber, maximum stress lower than material yield stress), as well as to the geometry of typical climbing holds. These reference dimensions and geometry were then optimized by FEM structural analysis. For the prototypes, a quenched steel alloy, 42CrMo4 (yield resistance 900 MPa) was selected.

The strain gauge locations and connections were designed to ensure a wide linear region of strains, cancel out the effect of bending and torque moments, and compensate for thermal drift. The sensor was designed based on a static analysis, taking yield as the failure criteria. The Von Mises yield criteria was selected to describe the onset of plasticity.

The device is composed of two parts, which are referred to as the beam and plate. The two parts are assembled through a bolt, which provides load continuity and enables for ease of disassembling the sensor.

The sensor was designed to withstand three times the maximum static load, which led to the consideration of a maximum load of 2000 N, applied 120 mm from the climbing wall. In

this condition, the safety factor is 1.1. Some data and indications related to the maximum possible load a hold can be subjected to during loading activity can be found in the literature, confirming that this maximum value is acceptable. Static lifting force values of approximately 600 N can be found in the works of Bourne et al. [15] and Amca et al. [16]. Dynamic test force values can also be found. For example, Fuss and Niegl [10] found that in dynamic jumping two hands dyno climbing, the maximum loads reached 1200 N. While analysing the motion of the center of mass during climbing, Zampagni et al. [17] collected interesting information about the dynamic distribution of vertical reaction forces under the feet. In the paper, the activity of many climbers is investigated, classified based on age, expertise, weight, etc. to identify the energy expenditure and energy optimization strategies. Both in static and dynamic exercise, the force exerted by hands and feet is generally lower than 0.6 times the weight. The authors conclude that the COM control can provide critical information on optimization of energy expenditure, stability and safety, but further investigations are required.

3.2. *FEM analysis*

The sensor design was optimized through iterative FEM analysis. Simulations were performed using ABAQUS 19.2 linear structural solver.

Linear static stress analysis was carried out using finite element model reproducing the real structure. All the structure parts were modelled using 2nd order solid elements. The mesh was made by HEX Solid Elements. Analytical stress assessment was based on element stresses. The model consists of 471276 nodes and 103356 elements. The 3-axis sensor component was verified under a tangential load of 2000 N, applied at 100 mm from the end of the beam at the opposite side from the fixed support. According to ASTM and UNI Standards [18, 19, 20] for dynamic ropes and climbing equipment, the maximum force that can be passed onto the climber in a very severe fall is 12 kN.

The Von Mises stress results can be observed in Figure 3. Maximum stress is close to the cantilever constraint and it is approximately 700 MPa, which is lower than material yield stress.

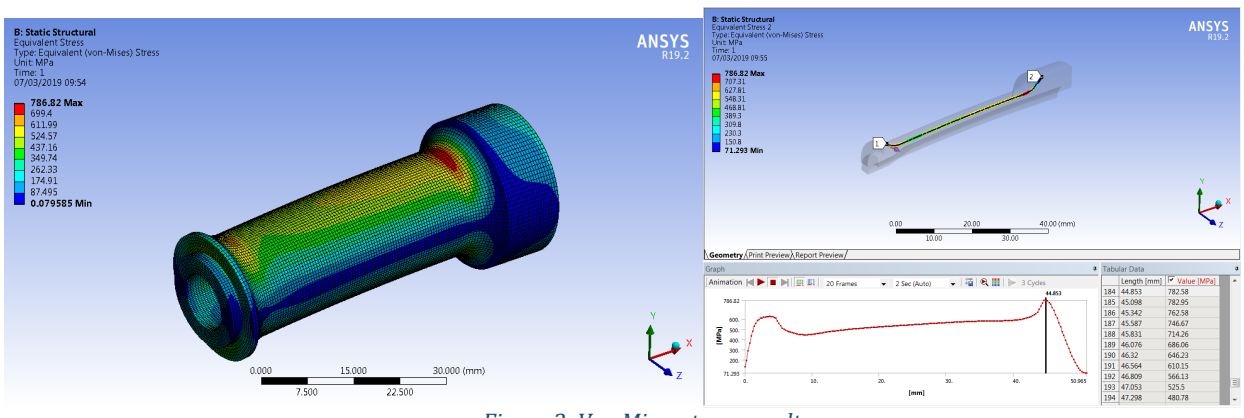

Figure 3: Von Mises stress results

3.3. Data acquistion system (DAQ) design

The chosen measuring range (2000 N), with a resolution of 10 N, imposed a lower limit of log2(200)=8 bit for the analog to digital converter (ADC) in charge of digitizing the signal coming from the strain gauge bridges. In the frequency domain, even though the literature provides little data regarding the dynamics of forces generated by a climber, as for example according to Saul et al. [21], a bandwidth of 5 Hz was estimated to be sufficient to capture most of the features that are likely to be relevant in the analysis of the climbing movement. The ADCs were therefore required to have a sampling rate of at least 10 Hz to satisfy the Nyquist-Shannon sampling theorem, and preferably higher to allow a suitable representation of the climber load in time. Commercial low cost information and communication technologies (ICTs) for weigh scale applications meet and exceed the above requirements.

Each sensor can be modelled as a structural element, with a beam equipped with strain gauges. The beam is connected to a set of three dedicated ADCs, one for each component of the force vector. The three ADCs are wired so as to work in parallel, minimizing the phase offset in the conversion of the three components of the force vector. Data from the three ADCs of a single sensor are collected by a microcontroller, which relays the data to the central processing unit via a cabled connection.

3.4. Computation of the Center of Mass (COM)

For the analysis, the global reference frame (XYZ) was defined as follows: the origin O is located at the bottom-left corner of the wall and the axes follow the right-hand rule, with the X and Y axes belonging to the plane of the wall. In this way, all positions in the 3D environment occupied by the athlete have positive coordinates. Medio-lateral forces (F_X) are positive rightwards, vertical forces (F_Y) are positive upwards and anteroposterior forces (F_Z) are positive when pointing away from the wall.

As mentioned in Section 1, the estimation of the *COM* trajectory γ of the entire body enables simplification in the study of articulated movements. In this frame, the laws of motion take the following form in Eqs. (1) and (2):

$$\vec{F} = m\vec{a}_G \tag{1}$$

$$\vec{\tau} = [I_G]\vec{\alpha} + \vec{\omega} \times [I_G]\vec{\omega} \tag{2}$$

where $\vec{F}$ is the total force applied to the body; m is the mass of the climbers; $\vec{a}_G$ is the *COM* acceleration; $\vec{\tau}$ is the total torque applied to the body; $[I_G]$ is the barycentric inertia tensor of the body; $\vec{\alpha}$ is the angular acceleration; and $\vec{\omega}$ is the angular velocity.

Both in static and dynamic exercise, the position of the *COM* ($\overrightarrow{R_G}$) can be retrieved by solving the torque equilibrium equation. However, when a dynamic exercise occurs, solving this equation would imply knowing $\vec{\omega}$, $\vec{\alpha}$ and $[I_G]$ for every time step.

To simplify the computation of $\overrightarrow{R_G}$, an experimental calibration protocol is proposed (see Section 4.5), consisting of two phases. In the first phase, named "*Setting*", the athlete is asked to grab onto four different holds and then keep a static position for 5 s; after this time, as soon as the athlete is given the start signal, the "Exercise" phase begins, with the climber performing prescribed movements on the instrumented wall. Similar to what is reported by

Quaine et al. [1, 3], the *COM* initial position ($\overrightarrow{R_{G_0}}$) is computed solving the torque equilibrium during the *Setting* phase, while during the *Exercise* phase, the Newton law provides the value of $\vec{a}_G$ for every time step. Integrating twice the acceleration and imposing proper initial conditions, the COM trajectory is precisely estimated.

These procedures present some criticalities. In particular, for the quasi-static condition required by the protocol, the equation of the total torque simplifies as shown in Eq. (3):

$$\vec{\tau} = 0 \tag{3}$$

Considering the defined reference system (Figure 2*b*), expanding the term of the total torque in terms of the force acting on the subject leads to a system composed of three scalar equations. However, as body weight $\overrightarrow{W} = -W \cdot u_y$ (where u_y is the versor of the y axis) does not exert any torque around the y axis, the system is underdetermined. Contrary to Quaine et al. [1] and to Noe et al. [3], where only the two components of the *COM* position vector lying on a transverse plane were evaluated, in this case the issue has been solved by adding a third independent equation. Combining the definition of the first moment of inertia S along the y axis with the equation of the translational equilibrium along the same y direction, a third independent equation is obtained, as shown in Eq. (5), leading to a determined system as shown in Eqs. (4-6):

$$\begin{cases} W \cdot z_G = +\sum_{i=1}^{N} F_i^y \cdot z_i - \sum_{i=1}^{N} F_i^z \cdot y_i & (4) \\ W \cdot y_G = \sum_{i=1}^{N} F_i^y \cdot y_i & (5) \\ W \cdot x_G = \sum_{i=1}^{N} F_i^y \cdot x_i - \sum_{i=1}^{N} F_i^x \cdot y_i & (6) \end{cases}$$

where N is the number of contacted holds; F_i^x, F_i^y, F_i^z are the components of the vector $\overrightarrow{F_i}$, the force exchanged between the athlete and the *i-th* hold; x_i, y_i, z_i are the components of the vector $\overrightarrow{R_i}$, which identifies the position of the *i-th* hold in the environment; x_G, y_G, z_G are the components of the vector $\overrightarrow{R_G}$.

The solution of this system yields the three components of the *COM* initial position vector ($\overrightarrow{R_{G_0}}$).

During the exercise phase, the Newton's force equilibrium equation is applied as shown in Eq. (7):

$$\sum_{i=1}^{N} \overrightarrow{F_i} - \overrightarrow{W} = m\vec{a}_G \tag{7}$$

gives the value of the *COM* acceleration for every time-step. Starting from the obtained $\vec{a}_G(t)$, COM velocity $\vec{v}_G(t)$ and position $\vec{R}_G(t)$ are computed as shown in Eqs. (8) and (9):

$$\vec{v}_G(t) = \int_0^t \vec{a}_G(t)\, dt \tag{8}$$

$$\vec{R}_G(t) = \int_0^t \vec{v}_G(t)\, dt + \overrightarrow{R_{G_0}} \tag{9}$$

For the integration, the trapezoid rule (Newton-Cotes closed formula of order one) has been used as shown in Eq. (10):

$$\int_a^b f(x)dx \approx \frac{b-a}{2}[f(a)+f(b)] \tag{10}$$

Mean and peak forces are extracted, both for every hold and overall values. In order to make comparisons between different subjects, they are normalized with respect to body weight.

For each sensorized hold, impulses are calculated following the definition shown in Eq. (11):

$$\Delta\overrightarrow{q_i} = \int_0^T \overrightarrow{F_i}\, dt \tag{11}$$

where $\Delta\overrightarrow{q_i}$ is the impulse caused by the force $\overrightarrow{F_i}$ exchanged between the athlete and the *i-th* hold and T is the contact time. Contact times for each hold are detected, checking that a vertical force is applied on it. The trapezoidal rule is used for numerical integration.

3.5. Performance indices

Many indices can be used to describe an athlete's activity and performance. In the present paper, the indices are obtained by means of processing force measurements.

Once the trajectory γ of the COM is obtained, work (L) and power (P) can be computed as shown in Eqs. (12) and (13):

$$L = \int_\gamma \sum_{i=1}^{N_{holds}} \vec{F}_i \cdot d\vec{s} \tag{12}$$

$$P = \sum_{i=1}^{N_{holds}} \vec{F}_i \cdot \vec{v}_G \tag{13}$$

However, as sport climbing is a discipline that implies many isometric contractions, these measures lead to an underestimation of the athlete's energy consumption. Energy expenditure is more fairly accounted for by using the four following performance indices.

Time-Averaged Effective Force (TAEF). This is the average over time of the sum of the force vector's moduli normalized to body weight. The Effective Force (*EF*) represents the sum of the force vector's moduli normalized to body weight as shown in Eq. (14), as a time-dependent quantity:

$$EF(t) := \frac{\sum_{i=1}^{N}\sqrt{F_i^{x^2}+F_i^{y^2}+F_i^{z^2}}}{W}, \tag{14}$$

where the TAEF is shown in Eq. (15):

$$TAEF := \frac{1}{T}\int_0^T EF(t)dt. \tag{15}$$

COM Effective Displacement (CED). Defined as the ratio between the in-plane component of the *COM* displacement and its total displacement during the exercise:

$$CED(t) = \frac{\sum_{i=1}^{N_{steps}-1} \sqrt{[x_G(i+1) - x_G(i)]^2 + [y_G(i+1) - y_G(i)]^2}}{\sum_{i=1}^{N} |\overrightarrow{R_G}(i+1) - \overrightarrow{R_G}(i)|} \quad (16)$$

Force Component Ratio (FCR). According to Quaine et al. [3], the *FCR* is the ratio between the sum of the moduli of the out-of-plane component of the force and the sum of the moduli of the in-plane component. This performance index can be computed as time-dependent or time-averaged (*TAFCR*) as shown in Eq. (17):

$$FCR(t) = \frac{\sum_{i=1}^{N} |F_i^z|}{\sum_{i=1}^{N} \sqrt{F_i^{x^2} + F_i^{y^2}}}; \; TAFCR = \frac{1}{T}\int_0^T FCR(t)dt \quad (17)$$

Hands to Feet Ratio (HFR). It is defined as the ratio between the mean forces exerted by upper and lower limbs on a static position as shown in Eq. (18):

$$HFR = \frac{\int_0^T (\overrightarrow{F_{LH}} + \overrightarrow{F_{RH}})}{\int_0^T (\overrightarrow{F_{LF}} + \overrightarrow{F_{RF}})} \quad (18)$$

The distribution of load between hands and feet, together with the application of out-of-plane forces, appears from previous studies to be correlated to the steepness of the route, as stated by Quaine et al. [3].

4. Experimental protocol

In order to assess the static characteristics of the measuring system, an experimental protocol, with four main properties, was defined.

The first property, accuracy, is the maximum deviation from the correct measure, obtained by means of repeated tests with different loads in different directions; this parameter is dependent on electric noise, thermal drift, point of application of the load. The second property, repeatability, is the maximum difference between repeated measurements, which is dependent on electric noise and thermal drift. The third property is resolution, which is the minimal variation of the input signal that can be measured. This is dependent on the geometry of the sensor and ADC resolution. The last property is stability, which is mainly dependent on temperature.

The experimental protocol consists of many sets.

4.1. First set: in plane force measurements

The four sensors were loaded with a constant 98 N load, in a plane parallel to the climbing wall (at an angle of 0°, 45°, 90°, 135°, and 180° with respect to the sensor's y axis (Figure 2*b*)), and along the sensor's axial direction (along the z axis). The sequence of measurement was repeated three times. The obtained strain measurements were compared with simulated values to validate the FEM model and verify the measuring performance. Furthermore, the strain measurements were processed to obtain the total force vector.

4.2. Second set: out of plane measurements

Three sets of measurements were run on axial force measurement sensor. 5 kg masses were hanged to the sensor, positioning the sensor parallel to the vertical direction and with a 45° angle to the vertical direction. The masses were added and removed to increment and decrement the total force. A total maximum mass of 50 kg and 25 kg were applied in the vertical and angled configuration, respectively. The measurements were then acquired for three cycles in loading and unloading for each configuration.

4.3. Third set: independence of the measurements value from the point of application of the force

In the third set, the independence of the measurements from the point of application of the force is investigated. As the in-plane component of the force induces bending stresses on the beam element, even a small misalignment in the positioning of the strain gages leads to measurement errors, as the circuit becomes sensitive to the applied moment instead of the force. A test was designed to check that the forces were correctly measured.

The procedure consists of two parts. In the first part, a 49 N weight is applied on the sensorised hold at three different hanging distances from the end of the beam (0 mm, 25 mm and 50 mm); in the second part two 49 N weights are hanged in two different positions, combining the previously listed distances from the sensor. Therefore, the load is not concentrated in a single point, but rather distributed between two points with the centre of load in between the points. The corresponding distributions are 0-25, 0-50 and 25-50 mm. In each condition, one measurement lasting 10 seconds with 10 Hz acquisition rate was performed.

4.4. Fourth set: COM position mesurement

The fourth set of experiments aims at evaluating the COM computation performance. The test was performed hanging three 49 N weights on the holds (Figure 4), leaving therefore one of them unloaded at each time, in order to simulate a tripedal stance. In these four cases, the COM position coordinates are the average of the coordinates of the three loaded holds, along each axis.

Figure 4: Testing wall with a 50 N weight hanged on each hold

4.5. Fifth set: full exercise

After separately testing the different components of the system, its performance has to be evaluated in a realistic situation. To ensure optimal conditions, subjects were asked to follow the experimental procedure as follows: the athletes started from a static quadrupedal position, then they were asked to complete four different tripedal stances, releasing one hold at a time and always returning to the quadrupedal position before reaching the new stance.

The four tripedal stances have been named T1, T2, T3 and T4. The five different configurations achieved in the exercise are schematically reported in Table 1 where RF, LF, RH and LH stand for right foot, left foot, right hand and left hand, respectively. The same configurations are shown in Figure 5.

Table 1: Configurations reached during the exercise

	Contacted holds			
Position	Hold 1	Hold 2	Hold 3	Hold 4
quadrupedal	RF	LF	RH	LH
T1	RF	LF	RH	
T2	RF	LF		LH
T3	RF		RH	LH
T4		LF	RH	LH

Figure 5: Tripedal stance configurations for full exercise tests

During the exercise, contact forces were acquired with the DAQ system and subsequently data were fully postprocessed with the developed code.

This procedure is analogous to procedures described by Fuss and Niegl [7].

5. Experimental results and discussion

In the following paragraphs, the results of each set of experiments are presented and discussed.

5.1. First set: in-plane force measurements

The results of the first set of experiments are reported in Figure 6 and 7.

Before any set of measurements, the holds were calibrated applying known weights and extracting the scaling coefficients (conversion factors between measured Voltage *(V)* and computed force *(F)*). The variation of scaling coefficients with different calibrations was monitored. In order for a measurement system to be considered stable, multiple measurements performed with the same external conditions over a significant time span had to produce the same results. This implies that the scaling coefficients have to show small variations in different set-ups of the wall.

The mean RMS noise on both channels was slightly less than the system resolution (1 N). In the two worst cases (x component channel of hold 4 and y component channel of hold 2), the noise was higher than the resolution by a very small amount. The standard deviation is limited and lower than 0.5 N, verifying the stability of the system. In fact, only the first hold shows a significant oscillation in the coupled noise with one value close to 2 N, which is probably an isolated case. It is remarkable that hold 3, which shows the lowest value of coupled noise, also exhibits the lowest variance in the scaling coefficients. The analysis of the recording of raw data coming from an unloaded hold (Figure 7) helps to investigate the main causes to the disturbances.

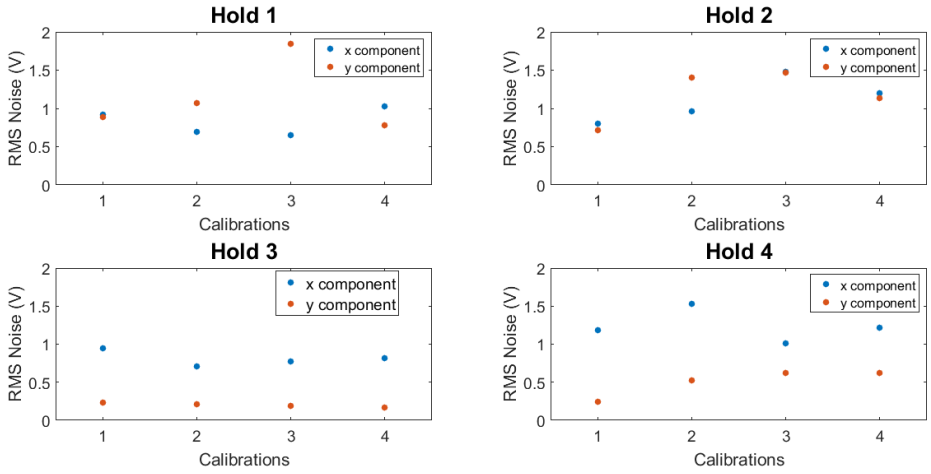

Figure 6: Accuracy measurement results - scatter plot for the RMS noise in different calibrations

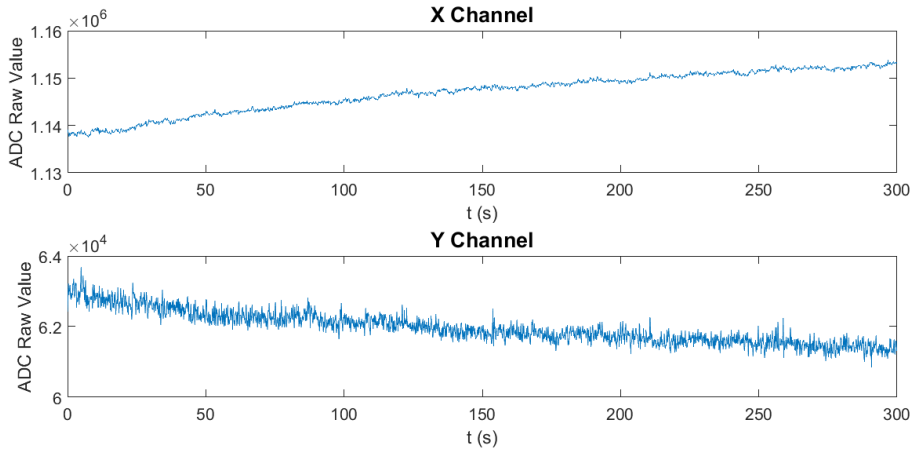

Figure 7: Stability measurements results - raw data acquisition

It emerges that the signals were affected by a low-frequency trend. This might be mainly due to the electrical fluctuations of the A/D converter, together with the thermal effects of the strain gages. In order to solve this issue, the software loaded on the acquisition boards automatically reset the offset when a significant variation of the signal is not observed over some seconds.

To examine the other noise contributions, the signals were processed in MATLAB®. The trend was removed using a high-pass Chebyshev filter of order 5 and cut off frequency equal to 0.2 Hz. The Power Spectral Density (PSD) was estimated for both signals by applying the Welch method with one-minute-long Hamming windows. Three parameters were extracted and considered for the analysis of amplitude and periodic behaviour of the signals: Average Rectified Value (ARV), Root Mean Square (RMS); and to estimate the mean of the PSD, the Mean Frequency (MNF) was selected. These parameters are indicated for the analysis of muscular activity, as for example by Gazzoni [21], Molinari [23] and Ashutosh [24].

The results are shown in Figure 8 and 9 and Table 2.

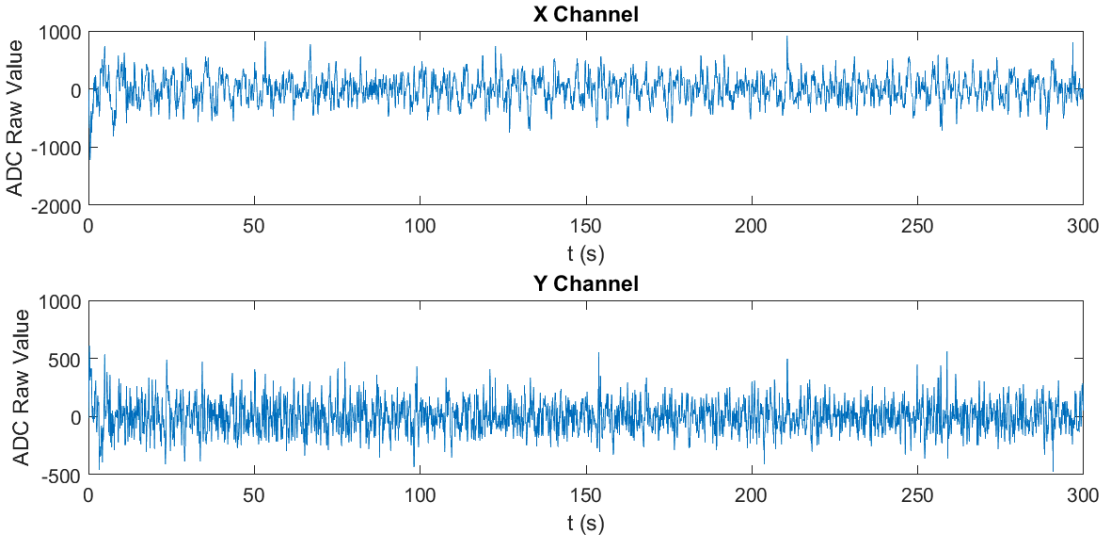

Figure 8: De-trended data

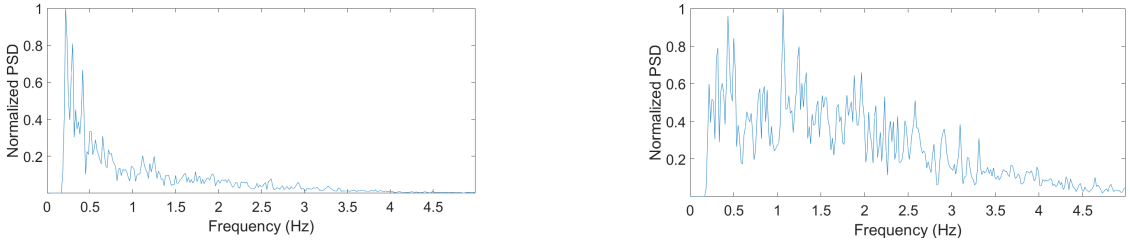

Figure 9: PSD of the de-trended signals, (a) X channel, (b) Y channel

Table 2: Time and frequency domain parameters.

	X channel	Y channel
ARV	173.1353	112.0713
RMS	218.5316	142.8147
MSF (Hz)	1.0881	1.7551

Since the analysed contribution is spread over all frequencies, it can be assumed to come from high-frequency disturbances, which are reflected in spurious frequencies because of aliasing (sample frequency is 10 Hz). However, the MNF is lower than the mean of the frequencies, showing that there is a prevalence in low frequencies, even after the removal of the principal trend. Considering the scaling coefficients, the RMS noise on the two channels corresponds to a force measurement error of some fractions of N. Thus, there is evidence that the system is efficiently shielded, as the pre-eminent contributions to the noise are given by thermal low-frequency fluctuations.

5.2. Second set: out of plane measurements

The measurements showed linearity with load (Figure 10), strong dependence on preloading and strong sensitivity to strain gauge misalignments in angled configuration measurements. While the measurements were reliable, linear and repeatable when the load is parallel to the axis of the beam (Figure 10 a), an hysteresis phenomenon occurs when

the direction of the load changes from parallel to angled with respect to axis of the beam (Figure 10 b).

The strain gauge positioning on out-of-plane force sensing devices requires particular precision. In future activities, particular attention will be devoted to define a procedure for reliable strain gauge positioning.

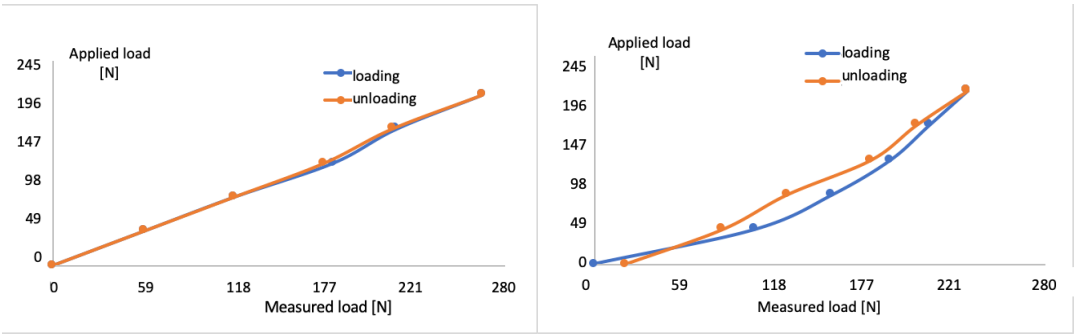

(a) *(b)*

Figure 10: Example of loading and unloading curves for out of plane measurements: case of forces (a) parallel to sensor axis and (b) 45° angled with respect to sensor axis

5.3. Third set: independence of the point of application of the force on the hold

The experiment was composed of two parts. In the first part, a single weight of 49 N was hanged at three different distances from the axis of the sensor, keeping the distance from the wall constant. In Table 3 and

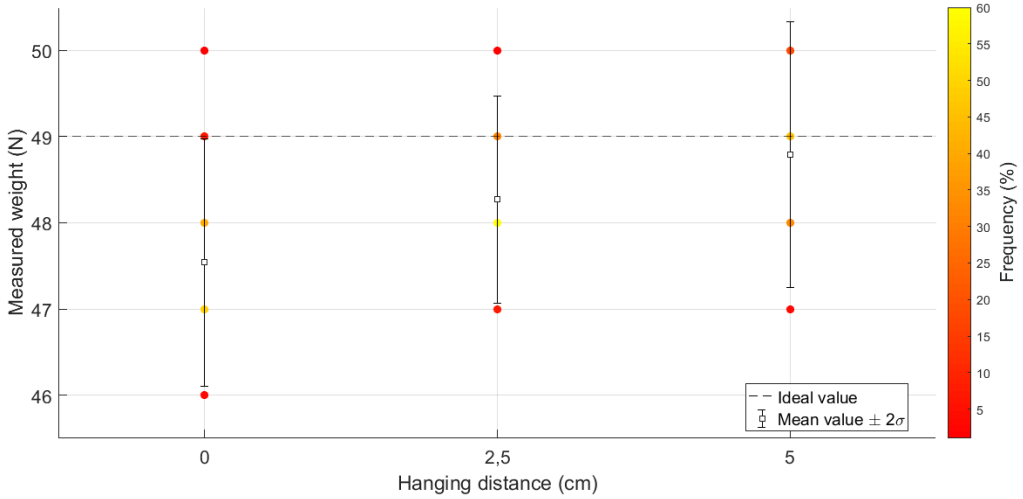

Figure 11, the results obtained for the first part of the experiment are reported. In the second part of the experiment, the weight was hung with varied length distributions along the axis of the sensor. This distribution length is measured with the zero positioned on the wall. The ideal output should be 49 N. The results corresponding to the second part of this experiment are reported in Table 4 and in Figure 12.

Table 3: Mean and standard deviation of the measurements (49 N) (100 samples on 10 sec measurements)

Hanging distance from sensor axis [mm]	0	25	50
Mean [N]	47.54	48.27	48.79
Standard Deviation [N]	0.7166	0.6006	0.7693

Table 4: Mean and standard deviation of the measurements (98 N) (100 samples on 10 sec measurements)

Hanging distance from wall [mm]	0-20	0-50	25-50
Mean [N]	96.81	97.33	98.06
Standard Deviation [N]	0.9816	1.1552	0.9081

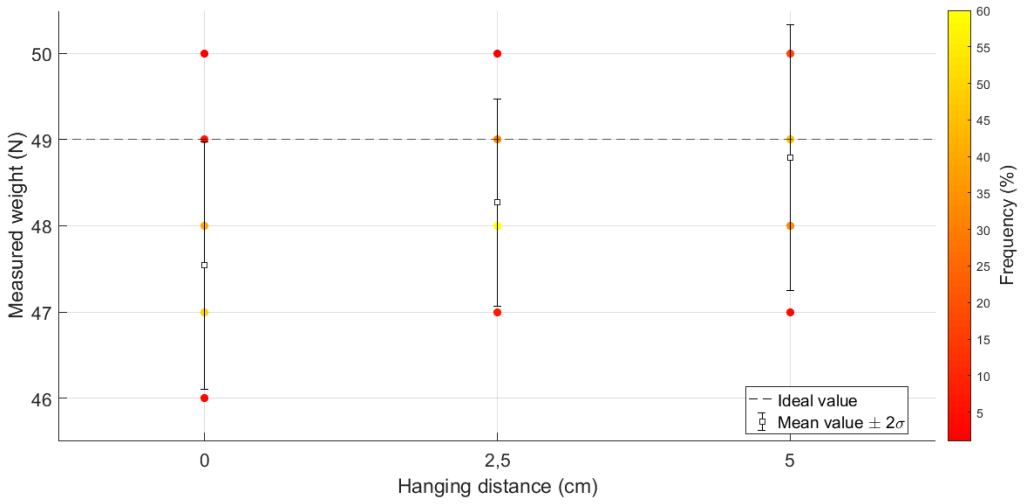

Figure 11: Scatter plot of the 100 readings, variable distance from sensor axis (49 N)

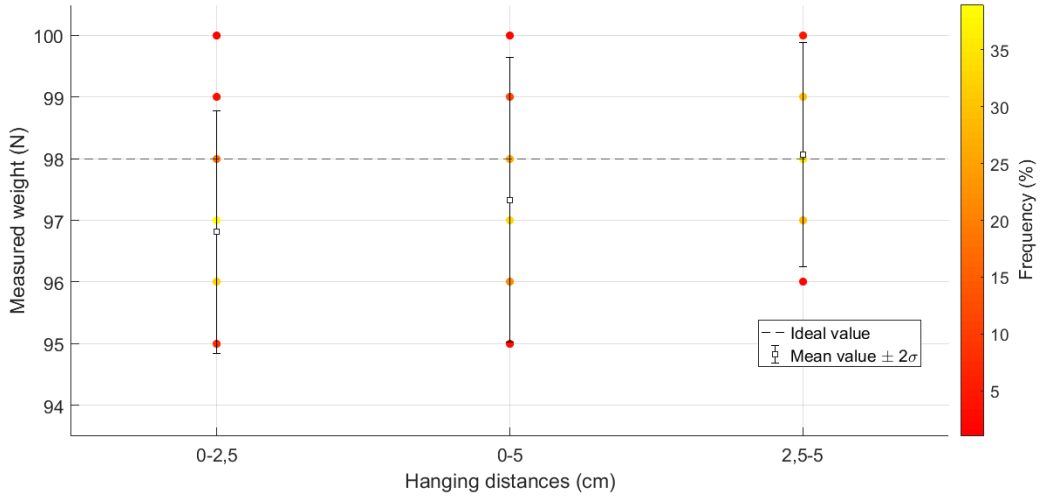

Figure 12: Scatter plot of the 100 readings, variable distance from wall (98 N)

The results show a small dependence of the load on the point of application. The maximum difference between the average of the measured values and the exact measurement (-1.46 N) is observed with the 49 N weight placed directly on the edge of the hold. However, considering the accuracy of the setup (±1 N) and the RMS noise on the channels, this discrepancy is negligible.

The second part of the test accounts for the fact that the holds hang some distance in mm away from the plane of the wall, therefore the load is not concentrated in a single point, but rather distributed. In this case, the ideal output is 98 N. The highest discrepancy (-1.19 N) is registered when the loads are hanged at the closest distances from the sensor. In this case too, it is comparable with the RMS noise on the sensor channels and the ideal value falls within the $\pm 2\sigma$ in all three loading configurations. For these reasons, the system is considered reliable, as different points of application of the loads lead to comparable results with an error of the same order of magnitude for the uncertainty of the system.

5.4. Fourth set: COM position

The COM position has been evaluated in a quasi-static situation, solving the torque equilibrium equation (Eqs. (4-6)) over subsequent time steps and averaging the results. In Table 5, the estimation error is reported.

Table 5: Estimation error obtained in the different tests

Configuration	Error modulus (mm)
Full	105.6
1	120.6
2	63.1
3	48.1
4	81.0
Mean	83.7
Standard Deviation	29.8

The different configurations have been named in this way: "Full" identifies when a weight is applied on all four holds, while numbers from 1 to 4 indicate which hold is left free at any time. The resulting mean error (83.7 mm) indicates that the estimation provides a good level of confidence. As the error is distributed on both the x and y coordinates, it is reasonable to think that the principal source of error is an incorrect measurement of contact forces, due to measurement noise.

The error on the initial COM position measurements can affect the following trajectory measurement, as it constitutes an incorrect initial condition. However, as the source has been identified in the noise superimposed on the signal, the correct functioning of the post-processing algorithm is ensured. A better insulation of the DAQ system will provide a sufficient condition for a more precise estimation.

5.5. Fifth set: full exercise

The exercise was performed by one male subject 1.75 m tall weighing approximately 650 N. The prescribed moves were completed in 26 s. After calibrating the system, the athlete performed a sequence and the corresponding performance parameters were obtained from data post-processing.

The main findings are reported in Table 6 and in Figure 13. The total range of motion of the COM remained below 1 m in both directions, with a small total planar displacement (1.5 m).

As it was expected from some results already reported in Noe et al. [3], the subject carries on strategies to minimize the oscillations of its COM. In order to maintain the equilibrium, forces are kept very close to the minimum possible, which is body weight. When the subject does not perform any dynamic move, the impulses and the contact times are low.

Table 6: Overall descriptive parameters extracted with the post-processing algorithm with mean and peak forces normalized to body weight

Elapsed Time [s]		26
COM Range of Motion [mm]	x component	614.3
	y component	747.3
COM In-plane Displacement [mm]		1544.4
Normalized Mean Force [N]	x component	-0.23
	y component	1.01
Normalized Peak Force [N]	x component	0.06
	y component	1.52
Work [J]		1589,3
Average Power [W]	1st method	61.125
	2nd method	55.440
TAEF		1.0181
HFR	x component	0.0325
	y component	0.3073

Time-Averaged Effective Force (TAEF)
Hands to Feet Ratio (HFR)

The distribution of weight among the limbs shows a net predominance of the feet, as the *HFR* is much smaller than 1 for both the computed components. In particular, the most meaningful for the analysis is the *y* component, which shows that the feet are applying an average force three times greater than the hands, thus supporting 75% of body weight.

The *EF* remains in general constant around unity, except for two opposite spikes, which are due to the adjustments in weight distribution performed when only one foot is in contact with the wall.

These results are a first estimation on the potentiality of the measuring system. Further research activity will be focused on the implementation and investigation on performance parameters during climbing activity.

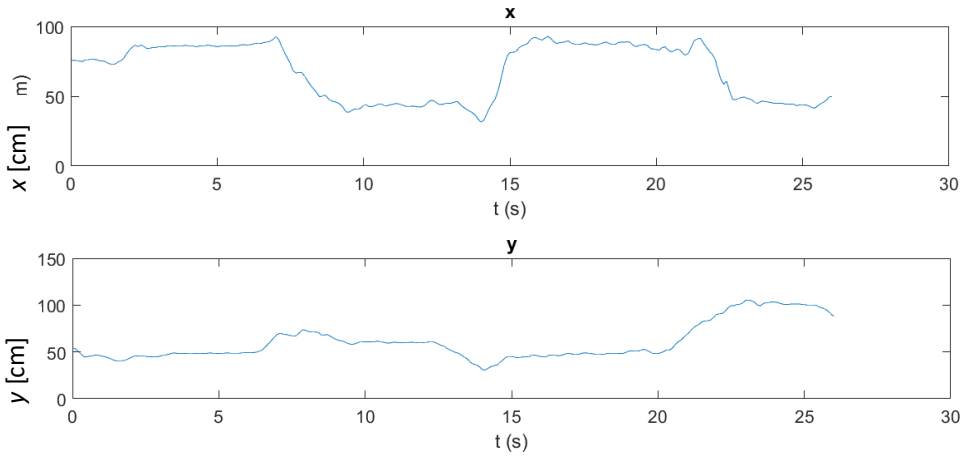

Figure 13: COM displacement along x and y direction

6. Conclusions

This work presents a novel, low-cost technology for the quantitative evaluation of sport climbing performance. The core of the technology is represented by the sensor, consisting of the hold supporting the modified bolt and equipped with force transducers. Instrumenting the wall, instead of the climber, causes no hindrance to movements during the practice, an appreciable advantage when considering the complexity of climbing moves.

The main objectives of this phase were the testing of the existent hardware, its refinement and the development from scratch of data processing algorithms. The accuracy and stability of the DAQ system have been proven. The scaling coefficient for the in-plane force measurement exhibited an appreciable variance between the holds. Nevertheless, the external electronic disturbances did not affect the measurements and the mean RMS value was maintained below the desired threshold, set equal to the measurement resolution (1 N). The in-plane force sensor tested for evidence that the desired sensitivity and resolution was obtained and the measurement was independent from the point of application of the force.

The DAQ system was completed, adding the sensor for the measurement of the out-of plane force component. Preliminary tests showed evidence regarding the linearity of the response produced by the sensor. Moreover, the sensitivity, which was lower than that of the in-plane measurements, appeared sufficient for the purpose, although it should be improved.

Data post-processing algorithms coded in MATLAB® allowed a biomechanical performance analysis of the exercise. They have been preliminarily tested with the 2D force measurement, applying a specific experimental protocol, conceived to foster the processing performances.

The precision in the estimation of the COM initial position fulfils the requirements. In fact, the source of the residual estimation error on COM initial positioning (about 80 mm) was identified in an incorrect force measurement due to the suboptimal environment in which tests were run.

For a quasi-static exercise involving multiple variations of configuration from a quadrupedal to a tripedal stance, all the quantities and parameters allowed by a 2D acquisition were effectively evaluated by the algorithm.

Due to the limited size of the wall used, the full exercise performed to test the complete system was not complex enough to completely assess the performances. A more demanding exercise, comprising also dynamical moves in which the athlete loses contact with the wall, will provide the condition for a more significant evaluation.

The rendering software developed in Python® offers readiness and stability of performances.

At the moment, forces are rendered by the display of vectors and by plots of the three components of the total force acting on the athlete. In the future, after the achievement of on-line data processing, a menu will be added to allow the selection of the information to display. These will include not only the mechanical properties (forces, velocity, acceleration, power, etc.), but also the time-dependent performance indicators.

Aknowledgments.

The authors thank RGTech (Torino, Itlay) and Ensinger Italia for counseling on materials and manufacturing of prototypes.

References

1. Quaine F, Martin L, Blanchi JP (1997) Effect of a leg movement on the organisation of the forces at the holds in a climbing position 3-D kinetic analysis. Human Movement Science 16:337-346
2. Quaine F, Martin L. (1999) A biomechanical study of equilibrium in sport rock climbing. Gait and Posture, 10:233-239
3. Noé F, Quaine F, Martin L (2001) Influence of steep gradient supporting walls in rock climbing: biomechanical analysis. Gait and Posture 13:86-94
4. Noé F , Quaine F, Martin L (2003) Mechanical effect of additional supports in a rocking on heels movement. Gait and Posture 18:78-84
5. Braghin F, Cheli F, Maldifassi S, Sabbioni E, Sbrosi M (2012) An Experimental Study of Climbers Performances Based on Hand-Grip Force Measurement. In: Allemang R., De Clerck J., Niezrecki C., Blough J. (eds) Topics in Modal Analysis II, Volume 6. Conference Proceedings of the Society for Experimental Mechanics Series. Springer, New York, NY, pp. 507-513
6. Fuss F K, Niegl G (2008) Instrumented climbing holds and performance analysis in sport climbing. Sports Technology 1(6):301–313. DOI: 10.1002/ jst. 71
7. Fuss F K, Niegl G (2008) The fully instrumented climbing wall: performance analysis, route grading and vector diagrams – A preliminary study. In: The Impact of Technology on Sport II, Taylor & Francis Group, London, UK, pp. 677-682
8. Delachanal J, Garnier D (2014) An aid to the practice of climbing on an artificial wall (Dispositif d'aide a la pratique de l'escalade sue un mur artificial), French Patent FR3017305A1, 11 February 2014

9. Lechner B, Filzwieser I, Lieschnegg M, Sammer P (2013) A Climbing Hold with an Integrated Three Dimensional Force Measurement and Wireless Data Acquisition. International Journal on smart sensing and intelligent systems, 6(5):2296-2307
10. Fuss FK, Niegl G (2010) Biomechanics of the two-handed dyno technique for sport climbing. Sports Eng, 13:19–30.
11. Tsang K F (2017) Climbing holds for use in rock climbing and rock climbing system. WIPO (PCT) Patent WO2017016246A1, February 2nd 2017
12. UNI EN 12572-3 – Artificial climbing structures Part 3: Safety requirements and test methods for climbing holds. WIPO (PCT) Patent WO/2019/123038. June 27th 2019.
13. Timoshenko, S., (1953), History of strength of materials, McGraw-Hill New York
14. International Patent (June 2019). *Sensorized device for fastening climbing holds provided with a triaxial load cell*. WO 2019/123038A1
15. Bourne R, Halaki M, Vanwanseele B, Clarke J. (2011) Measuring lifting forces in rock climbing: effect of hold size and fingertip structure. J Appl Biomech, 27(1):40-46.
16. Amca AM, Vigouroux L, Aritan S, Berton E. Effect of hold depth and grip technique on maximal finger forces in rock climbing (2012) J Sport Sci, 30(7):669e-677. https://doi.org/10.1080/02640414.2012.658845
17. Zampagni ML, Brigadoi S, Schena F, Tosi P, Ivanenko YP. (2011) Idiosyncratic control of the center of mass in expert climbers. Scand J Med Sci Sports, 21(5):688-699. https://doi.org/10.1111/j.1600-0838.2010.01098.x.
18. ASTM F1774 – 13 - Standard Specification for Climbing and Mountaineering Carabiners
19. UNI EN 959 – Mountaneering Equipment – Rock anchors – Safety requirements and test methods
20. ASTM F887 – 18 - Standard Specifications for Personal Climbing Equipment
21. Saul D, Steinmetz G, Lehmann W, Schilling AF (2019) Determinants for success in climbing: A systematic review. Journal of Exercise Science & Fitness, 17(3):91-100, https://doi.org/10.1016/j.jesf.2019.04.002.
22. Gazzoni M, "Bioengineering of phisical training and of sport" (in Italian) Master Thesis, Politecnico di Torino, A.A. 2017/2018.
23. Molinari F, "Biomedical data processing" in Italian) Master Thesis, Politecnico di Torino, A.A. 2016/2017.
24. Ashutosh G, Tabassum S, Ridhi G, Richa S (2017) Emg Signal Analysis of Healthy and Neuropathic Individuals, 2017 IOP Conf. Ser.: Mater. Sci. Eng. 225, 1.